

This paper describes objective technical results and analysis. Any subjective views or opinions that might be expressed in the paper do not necessarily represent the views of the U.S. Department of Energy or the United States Government

Dispersive Fourier transformation for megahertz detection of coherent Stokes and anti-Stokes Raman spectra

Alexis Bohlin,¹ Brian D. Patterson,¹ and Christopher J. Klier^{1*}

Sandia National Laboratories, Livermore, CA 94551

**Corresponding author: cjkliew@sandia.gov*

Received Month X, XXXX; revised Month X, XXXX; accepted Month X, XXXX; posted Month X, XXXX (Doc. ID XXXXX); published Month X, XXXX

In many fields of study, from coherent Raman microscopy on living cells to time-resolved coherent Raman spectroscopy of gas-phase turbulence and combustion reaction dynamics, the need for the capability to time-resolve fast dynamical and nonrepetitive processes has led to the continued development of high-speed coherent Raman methods and new high-repetition rate laser sources, such as pulse-burst laser systems. However, much less emphasis has been placed on our ability to detect shot to shot coherent Raman spectra at equivalently high scan rates, across the kilohertz to megahertz regime. This is beyond the capability of modern scientific charge coupled device (CCD) cameras, for instance, as would be employed with a Czerny-Turner type spectrograph. As an alternative detection strategy with megahertz spectral detection rate, we demonstrate dispersive Fourier transformation detection of pulsed (~ 90 picosecond) coherent Raman signals in the time-domain. Instead of reading the frequency domain signal out using a spectrometer and CCD, the signal is transformed into a time-domain waveform through dispersive Fourier transformation in a long single-mode fiber and read-out with a fast sampling photodiode and oscilloscope. Molecular *O*- and *S*-branch rotational sideband spectra from both N_2 and H_2 were acquired employing this scheme, and the waveform is fitted to show highly quantitative agreement with a molecular model. The total detection time for the rotational spectrum was 20 nanoseconds, indicating an upper limit to the detection frequency of ~ 50 MHz, significantly faster than any other reported spectrally-resolved coherent Raman detection strategy to date.

Coherent anti-Stokes Raman spectroscopy (CARS) is today employed in a variety of research applications, such as cell biology [1], combustion diagnostics [2], and the standoff detection of explosives [3]. It is the combination of excellent chemical selectivity, i.e. the ability to probe distinct quantum states of individual molecular species, and the coherent properties of the generated signal beam, that make this technique very powerful. For many applications, rapidly changing systems, with characteristic time-scales ranging from μs to ms require that measurements are performed nearly instantaneously, ideally within a single shot of a short-pulsed laser. This is a unique strength of Raman-based spectroscopies, as it is the time-duration of the probe pulse which ultimately limits the temporal resolution of the technique. Thus, users of coherent Raman spectroscopies have long been able to “freeze” dynamics of interest by recording data from a single laser shot. Statistics can then be built up from single realizations of the measured physical scalar, such as the instantaneous molecular temperature or concentration, as evaluated from the measured molecular spectrum. However, to follow time-correlated dynamics of a system which is evolving on the time scale of μs , the spectral detection strategy must also be capable of a very high refresh rate, in the megahertz regime [4]. Cutting-edge CMOS camera technologies are now capable of 1 MHz detection frame rates when operated in a cropped array mode with ~ 128 active pixels across the chip for spectral detection. Such systems are also limited to 12-bit depth, while the squared dependence on molecular density for coherent Raman spectroscopy often requires 14- or 16-bit depth for sufficient dynamic range. Line-scan CCD cameras have been demonstrated for continuous spectral measurements at 100-kHz, for example, in transient absorption spectroscopy experiments [5]. Faster CCD detection rates may be possible with multi-frame CCD options [4, 6], but such technologies are limited by the physical

framing built into the camera to ~ 10 's of frames and also suffer from blooming effects as the charge is transferred through the storage array, reducing the quantitative accuracy of stored data.

Another option, the topic of the current work, is to consider frequency-resolved spectral detection performed in the time-domain by the technique of dispersive Fourier transformation (DFT) [7]. The basic idea, depicted in Fig. 1, is to send the pulsed broadband CARS signal through a long fiber where the intrinsic group velocity dispersion (GVD) of the medium acts to spectrally separate the different wavelengths of the signal. The discretized spectral components are then registered with a fast single-pixel detector sampling read-out and get classified based on their arrival time, in the same manner as a classic time-of-flight instrument. This detection scheme has been proposed in connection to fiber dispersion

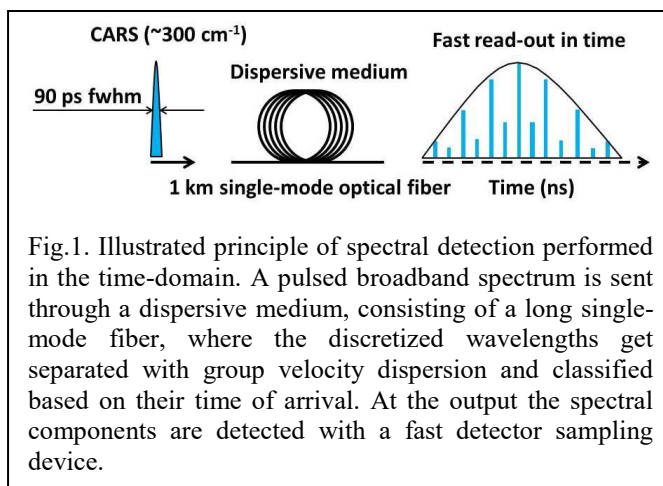


Fig. 1. Illustrated principle of spectral detection performed in the time-domain. A pulsed broadband spectrum is sent through a dispersive medium, consisting of a long single-mode fiber, where the discretized wavelengths get separated with group velocity dispersion and classified based on their time of arrival. At the output the spectral components are detected with a fast detector sampling device.

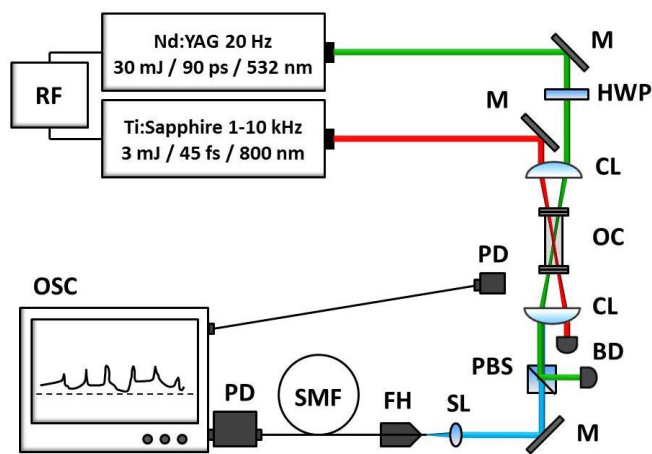


Fig. 2. Experimental setup for generating coherent rotational Raman signals and time-domain fiber dispersion detection strategy. M – mirror, HWP – half wave plate, CL- cylindrical lens, OC – optical cell, BD – beam dump, PBS – polarizing beam splitter cube, SL – spherical lens, FH – fiber holder, SMF – single-mode fiber, PD – photo diode, OSC – oscilloscope, RF – 100 MHz radio frequency master clock.

measurements [8], and variants of the same scheme have been explored in optical sensing applications [9-11], where molecular absorption spectra resulting from supercontinuum wavelength sweeps are mapped as waveforms in the time-domain. Instead, in the current work, it is the fact that the signal pulse in a CARS experiment will mimic the time-behavior of the probe pulse, i.e., a short or ultra-short pulse of light which contains the frequency-resolved coherent Raman spectrum, which allows the use of DFT to frequency-resolve the signal spectrum via chromatic dispersion in time with fast detection.

The generation of the coherent Raman signal was performed with time synchronized femtosecond (fs) and picosecond (ps) laser systems configured in a hybrid fs pump ps probe setup [12, 13], displayed in Fig.2. The fs laser system consisted of an oscillator (KM Labs, Halcyon) synced to an external 100 MHz radio frequency (RF) source acting as a master clock. The oscillator pumped a fs regenerative amplifier (KM Labs, Wyvern 1000), producing output pulses of 45 fs full-width at half maximum (fwhm) centered at a wavelength of ~ 800 nm, and operated at about 3mJ/pulse with a rate of 1kHz.

The ps laser system consisted of a 20 Hz regenerative amplified mode-locked Nd:YAG laser, with a seed laser phase-locked to the same external 100 MHz RF source, allowing for precise electronic timing between the fs and ps pulses at the experiment with sub-ps jitter. The output of the frequency doubled Nd:YAG at 532 nm was ~ 30 mJ/pulse with a pulse duration of approximately 90 ps fwhm. The laser beams were setup in a crossed two-beam configuration [14], with small enough incident angle [15] to achieve near perfect phase-matching condition for all the involved transitions (< 360 cm^{-1}) of this study. An optical cell was placed at the crossing in order to generate signals from pure gas-mixtures of two separate molecules, N_2 and H_2 . The coherent Raman scattered signals of both the species, containing rotational sidebands from Stokes and anti-Stokes shifted light, respectively, were isolated from the probe beam using a polarization gating technique [14]. The signal beam was injected via a $f=25$ mm focusing lens into a 1 km long single-mode (SM) optical fiber (Nufern, 460-HP) placed on a high finesse x-y-z pedestal stage. An FC-connector mounted at the end of the fiber channeled the dispersed light into a high-speed unamplified photodiode detector (Picometrix, D-15-FC), having an impulse response of 15 ps full duration at half maximum (fdhm). The photodiode output was finally digitalized using a 6 GHz bandwidth digital storage oscilloscope (Tektronix, TDS6604) with a 20 GS/s sample rate for single-shot acquisition of the signal waveform. The recordings were started at a

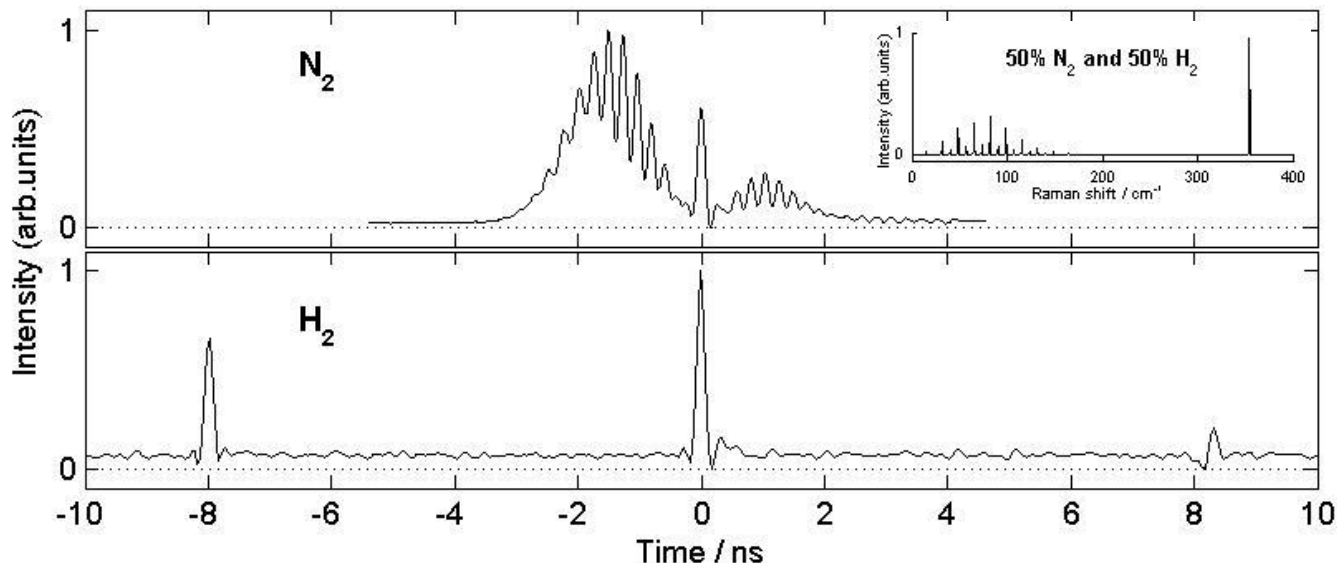


Fig. 3. Coherent Raman signals from (a) N_2 and (b) H_2 detected as waveforms in the time-domain, using a long optical fiber and fast detector sampling device described in the text. The spectrally dispersed *O*- and *S*-branch transitions corresponding from red- and blue shifted light, respectively, have different arrival times relative the zero-shift light from the remaining probe beam. The data presented have been averaged from 10 instantaneous measurements. In the insert, a rotational CARS spectrum recorded in a mixture with 50% N_2 and 50% H_2 using a standardized spectral detection scheme, is shown.

fixed delay, triggered from the output of a photodiode (EOT ET-

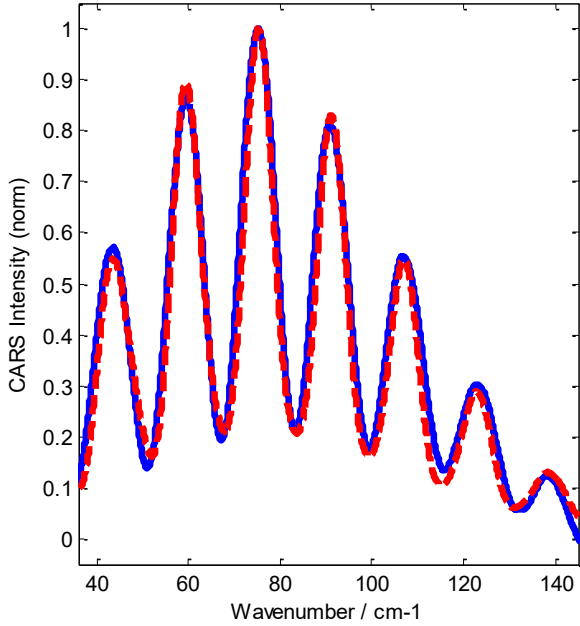


Fig. 4. (Blue) Measured CARS spectrum of N_2 at 295 K, as detected through the DFT detector. The time axis has been converted to Raman shift by accounting for the dispersion of the fiber. The total detection time is 20 nanoseconds. (Red) The simulated CARS spectrum of N_2 at 295 K, convolved with the instrument response function of the current DFT spectrometer. Quantitative spectral agreement is demonstrated.

3500) placed near the signal generation plane.

The transformation of the frequency-resolved CARS signal pulse into a time-domain waveform through the fiber is given by $\Delta\tau = |D|z\Delta\lambda$, where D is the GVD of the dispersive element, which was measured to be $D = 496 \text{ ps nm}^{-1} \text{ km}^{-1}$, $\Delta\lambda$ is the bandwidth of the signal pulse and z is the propagation distance in the fiber. The maximum spectral resolution of the current DFT instrument is thus limited by the detection bandwidth of our 6 GHz oscilloscope, as both the total fiber dispersion and fast photodiode could provide resolution approximately one order of magnitude greater than could be detected on the oscilloscope. However, as shown below, the acquired resolution was sufficient for quantitative fitting of the molecular spectrum to evaluate the N_2 rotational temperature.

Figure 3 displays the results from the sampling of coherent rotational Raman signals recorded in pure gas-phase samples of N_2 (a) and H_2 (b). The acquisitions shown were slightly averaged from 10 instantaneous measurements, to reduce contributions from the detector noise. The detected waveforms show distinct dispersed spectral components, from both the O ($\Delta J = -2$) and S ($\Delta J = 2$) branch rotational sidebands, where J denotes the rotational quantum number of the molecules. In the context of a non-linear technique, the O and S branches correspond to redshifted (Stokes) and blueshifted (anti-Stokes) light, respectively, relative to the fixed wavelength of the probe beam. Therefore, in Fig. 3, with positive dispersion of the optical fiber, the coherent Stokes Raman scattered light (CSRS) arrives before the CARS light, and accordingly have been assigned negative times relative the zero-shift probe beam, detected at time zero. Note, that the remaining probe light has been transmitted intentionally through the system to be used as a point of reference.

Otherwise, the polarization gating of the two-beam rotational CARS technique can easily achieve a $1:10^6$ suppression of the probe beam. In the insert of Fig. 3 a rotational CARS spectrum is shown recorded in a mixture with 50% N_2 and 50% H_2 as a result from a previous work [16]. In Ref. [16] a standardized detection was employed, implemented with a Czerny-Turner type imaging spectrograph and a CCD camera. The overall spectral features of both the schemes can be compared immediately and qualitative agreement is observed; with approximately 8 clearly resolved lines from the N_2 even parity transitions populated at 295 K. The distance between two points in the temporal profile, i.e. between any of the transitions in the N_2 envelope and the first H_2 - S_0 transition, is mapped approximately linearly to the same reference features within the spectrum. This indicates a nearly first order dispersion of the fiber, also verified by the observation that the separation between the spectral lines increased by a factor of two when doubling the length of the fiber.

In Fig. 4, the N_2 CARS spectrum collected from the fiber DFT spectrometer, collected at 295 K, has been fitted using a time-domain N_2 molecular model for CARS which we have used previously [17] and which has been previously validated [12]. Higher order dispersion of the CARS signal through the fiber in the DFT spectrometer, while small, was accounted for by fitting the known CARS transition frequencies to a 5th-order polynomial with regard to DFT delay time. The simulated N_2 spectrum at 295 K was convolved in the frequency domain with the instrument response function of the current DFT spectrometer, which was measured using the Raleigh scattering line without CARS contributions. The calculated spectrum was multiplied by a normalized nonresonant CARS spectrum recorded in argon, to correct for the excitation efficiency of our fs laser across the signal bandwidth of interest. Such fitting procedure is adequate subject to the assumption that a full transformation of the frequency-domain spectrum into a time-domain waveform [18] has been achieved, and that the resolution is indeed limited by the detection bandwidth of the oscilloscope. As shown in Fig. 4, indeed, the spectrum collected with the DFT detector is thus well fitted at 295 K, and demonstrates excellent spectral contour agreement. The total collection time for the spectrum was 20 nanoseconds, at which point the photodiode and oscilloscope were ready for the next series of data. At this rate, rotational Raman spectra could be obtained at a rate of up to 50 MHz with quantitative accuracy. The repetition rate of our lasers does not permit demonstration of repeated shots at this frame rate, but current efforts in pulsed burst-mode lasers [19] will soon enable such measurements, and here we are presenting a capable detection strategy for coherent Raman signals generated well into the MHz repetition rate regime.

The intention of this work was to explore an interesting spectral detection scheme for pulsed broadband coherent Raman signals employed in the time-domain which is capable of very fast detection scan rates, and to assess the viability of using fiber dispersion of a coherent pulsed signal as opposed to a standard spectrometer and CCD combination for quantitative spectral analysis. We have demonstrated the concept of using fiber dispersion to separate a frequency dependent CARS signal in time. Several significant improvements should be made to optimize the setup for applied measurements. A significant benefit of the method of DFT spectral detection, which we plan to explore in a future publication, is the capability to amplify the signal through stimulated Raman gain inside the fiber element, which can compensate for the attenuation of the signal waveform as it propagates through the long fiber [20]. For single-mode propagation of the signal presented here, which is centered at 532 nm, a fiber with a 2.5 μm core and 30 dB/km attenuation was required. However, the frequency of the probe beam

in a CARS process only acts as the carrier frequency for the signal, and can therefore be tuned to enable the use of fibers with a better dispersion-to-loss ratio. For instance, DFT with stimulated Raman amplification of signals within the fiber has been demonstrated at 800 nm [20]. By using a probe beam with a wavelength in the near IR, standard single mode telecom fibers can be used, which often have attenuation on the order of 0.25 dB/km, over 100 times less than in fiber for single mode propagation of 532 nm light. Further, in this case the core diameter of the fiber is also dramatically increased, which makes the injection of signal light into the core more facile. Lastly, by using an oscilloscope with significantly higher bandwidth, such that the limiting factor in the resolution of the detection technique should become the fast photodiode, the same resolution obtained here could be obtained with approximately one tenth the length of fiber used, reducing the signal attenuation by 10 fold.

Funding. This work was supported by the Division of Chemical Sciences, Geosciences, and Biosciences, the Office of Basic Energy Sciences (BES), the U.S. Department of Energy (DOE). Sandia National Laboratories is a multi-mission laboratory managed and operated by Sandia Corporation, a wholly owned subsidiary of Lockheed Martin Corporation, for the DOE's National Nuclear Security Administration under contract DE-AC04-94AL85000.

1. A. Zumbusch, G. R. Holtom, and X. S. Xie, *Phys. Rev. Lett.* **82**, 4142-4145 (1999).
2. S. Roy, J. R. Gord, and A. K. Patnaik, *Prog. Energy Combust. Sci.* **36**, 280-306 (2010).
3. M. T. Bremer, P. J. Wrzesinski, N. Butcher, V. V. Lozovoy, and M. Dantus, *Appl. Phys. Lett.* **99** (2011).
4. P. F. Wu, W. R. Lempert, and R. B. Miles, *Aiaa J.* **38**, 672-679 (2000).
5. F. Kanal, S. Keiber, R. Eck, and T. Brixner, *Opt. Express* **22**, 16965-16975 (2014).
6. L. Lazovsky, D. Cismas, G. Allan, and D. Given, "Ccd sensor and camera for 100 mfps burst frame rate image capture," in *Proc. SPIE 5787*(2005), pp. 184-190.
7. K. Goda, and B. Jalali, *Nat Photon* **7**, 102-112 (2013).
8. Y. C. Tong, L. Y. Chan, and H. K. Tsang, *Electron. Lett.* **33**, 983-985 (1997).
9. P. V. Kelkar, F. Coppinger, A. S. Bhushan, and B. Jalali, *Electron. Lett.* **35**, 1661-1662 (1999).
10. S. T. Sanders, *Appl. Phys. B-Lasers Opt.* **75**, 799-802 (2002).
11. J. Hult, R. S. Watt, and C. F. Kaminski, *Opt. Express* **15**, 11385-11395 (2007).
12. J. D. Miller, S. Roy, M. N. Slipchenko, J. R. Gord, and T. R. Meyer, *Opt. Express* **19**, 15627-15640 (2011).
13. S. P. Kearney, and D. J. Scoglietti, *Opt. Lett.* **38**, 833-835 (2013).
14. A. Bohlin, B. D. Patterson, and C. J. Kliewer, *J. Chem. Phys.* **138** (2013).
15. A. Bohlin, and C. J. Kliewer, *The Journal of Chemical Physics* **138**, 221101-221104 (2013).
16. A. Bohlin, E. Nordstrom, B. D. Patterson, P. E. Bengtsson, and C. J. Kliewer, *J. Chem. Phys.* **137** (2012).
17. A. Bohlin, and C. J. Kliewer, *The journal of physical chemistry letters* **6**, 643-649 (2015).
18. K. Goda, D. R. Solli, K. K. Tsia, and B. Jalali, *Phys. Rev. A* **80**, 12 (2009).
19. S. Roy, P. S. Hsu, N. Jiang, M. N. Slipchenko, and J. R. Gord, *Opt. Lett.* **40**, 5125-5128 (2015).
20. K. Goda, A. Mahjoubfar, and B. Jalali, *Appl. Phys. Lett.* **95**, 3 (2009).

REFERENCES

1. A. Zumbusch, G. R. Holtom, and X. S. Xie, "Three-dimensional vibrational imaging by coherent anti-Stokes Raman scattering," *Phys. Rev. Lett.* **82**, 4142-4145 (1999).
2. S. Roy, J. R. Gord, and A. K. Patnaik, "Recent advances in coherent anti-Stokes Raman scattering spectroscopy: Fundamental developments and applications in reacting flows," *Prog. Energy Combust. Sci.* **36**, 280-306 (2010).
3. M. T. Bremer, P. J. Wrzesinski, N. Butcher, V. V. Lozovoy, and M. Dantus, "Highly selective standoff detection and imaging of trace chemicals in a complex background using single-beam coherent anti-Stokes Raman scattering," *Appl. Phys. Lett.* **99**(2011).
4. P. F. Wu, W. R. Lempert, and R. B. Miles, "Megahertz pulse-burst laser and visualization of shock-wave/boundary-layer interaction," *AIAA J.* **38**, 672-679 (2000).
5. F. Kanal, S. Keiber, R. Eck, and T. Brixner, "100-kHz shot-to-shot broadband data acquisition for high-repetition-rate pump-probe spectroscopy," *Opt. Express* **22**, 16965-16975 (2014).
6. L. Lazovsky, D. Cismas, G. Allan, and D. Given, "CCD sensor and camera for 100 Mfps burst frame rate image capture," in *Proc. SPIE 5787* (2005), 184-190.
7. K. Goda and B. Jalali, "Dispersive Fourier transformation for fast continuous single-shot measurements," *Nat Photon* **7**, 102-112 (2013).
8. Y. C. Tong, L. Y. Chan, and H. K. Tsang, "Fibre dispersion or pulse spectrum measurement using a sampling oscilloscope," *Electron. Lett.* **33**, 983-985 (1997).
9. P. V. Kelkar, F. Coppinger, A. S. Bhushan, and B. Jalali, "Time-domain optical sensing," *Electron. Lett.* **35**, 1661-1662 (1999).
10. S. T. Sanders, "Wavelength-agile fiber laser using group-velocity dispersion of pulsed super-continua and application to broadband absorption spectroscopy," *Appl. Phys. B-Lasers Opt.* **75**, 799-802 (2002).
11. J. Hult, R. S. Watt, and C. F. Kaminski, "High bandwidth absorption spectroscopy with a dispersed supercontinuum source," *Opt. Express* **15**, 11385-11395 (2007).
12. J. D. Miller, S. Roy, M. N. Slipchenko, J. R. Gord, and T. R. Meyer, "Single-shot gas-phase thermometry using pure-rotational hybrid femtosecond/picosecond coherent anti-Stokes Raman scattering," *Opt. Express* **19**, 15627-15640 (2011).
13. S. P. Kearney and D. J. Scoglietti, "Hybrid femtosecond/picosecond rotational coherent anti-Stokes Raman scattering at flame temperatures using a second-harmonic bandwidth-compressed probe," *Opt. Lett.* **38**, 833-835 (2013).
14. A. Bohlin, B. D. Patterson, and C. J. Kliewer, "Communication: Simplified two-beam rotational CARS signal generation demonstrated in 1D," *J. Chem. Phys.* **138**(2013).
15. A. Bohlin and C. J. Kliewer, "Communication: Two-dimensional gas-phase coherent anti-Stokes Raman spectroscopy (2D-CARS): Simultaneous planar imaging and multiplex spectroscopy in a single laser shot," *The Journal of Chemical Physics* **138**, 221101-221104 (2013).
16. A. Bohlin, E. Nordstrom, B. D. Patterson, P. E. Bengtsson, and C. J. Kliewer, "Direct measurement of S-branch N_2-H_2 Raman linewidths using time-resolved pure rotational coherent anti-Stokes Raman spectroscopy," *J. Chem. Phys.* **137**(2012).
17. A. Bohlin and C. J. Kliewer, "Direct coherent Raman temperature imaging and wideband chemical detection in a hydrocarbon flat flame," *The journal of physical chemistry letters* **6**, 643-649 (2015).
18. K. Goda, D. R. Solli, K. K. Tsia, and B. Jalali, "Theory of amplified dispersive Fourier transformation," *Phys. Rev. A* **80**, 12 (2009).
19. S. Roy, P. S. Hsu, N. Jiang, M. N. Slipchenko, and J. R. Gord, "100-kHz-rate gas-phase thermometry using 100-ps pulses from a burst-mode laser," *Opt. Lett.* **40**, 5125-5128 (2015).
20. K. Goda, A. Mahjoubfar, and B. Jalali, "Demonstration of Raman gain at 800 nm in single-mode fiber and its potential application to biological sensing and imaging," *Appl. Phys. Lett.* **95**, 3 (2009).